Bioorganic & Medicinal Chemistry 17 (2009) 5038–5043

Contents lists available at ScienceDirect

Bioorganic & Medicinal Chemistry

journal homepage: www.elsevier.com/locate/bmc

Ruthenium complexes endowed with potent anti-*Trypanosoma cruzi* activity: Synthesis, biological characterization and structure–activity relationships

Claudio Luis Donnici [a,*], Maria Helena Araújo [a], Henrique S. Oliveira [a], Diogo Rodrigo Magalhães Moreira [b], Valéria R. Alves Pereira [c], Marina de Assis Souza [c], Maria Carolina Accioly Brelaz de Castro [c], Ana Cristina Lima Leite [b,*]

[a] *LASELORG-QUIM—Laboratório de Síntese, Eletrossíntese Orgânica e Química Medicinal, Departamento de Química, ICEX, Universidade Federal de Minas Gerais (UFMG), 31270-901, Belo Horizonte—MG, Brazil*
[b] *LABSINFA—Laboratório de Planejamento, Avaliação e Síntese de Fármacos, Departamento de Ciências Farmacêuticas, Universidade Federal de Pernambuco (UFPE), 50740-520, Recife—PE, Brazil*
[c] *Laboratório de Imunogenética, Departamento de Imunologia, Centro de Pesquisas Aggeu Magalhães, Fundação Oswaldo Cruz (FIOCRUZ), 50670-420, Recife—PE, Brazil*

ARTICLE INFO

Article history:
Received 31 March 2009
Revised 25 May 2009
Accepted 27 May 2009
Available online 17 June 2009

Keywords:
Trypanosoma cruzi
Metal complexes
Ruthenium
Thiazole
Hydrazone
DNA interaction

ABSTRACT

Although effective against epimastigotes (proliferative form) and of low cytotoxicity in mammals, the aryl-4-oxothiazolylhydrazones (ATZ) display only limited activity against trypomastigotes (bloodstream form) of *Trypanosoma cruzi*. Considering the metal complexation approach with bioactive ligands as one possible strategy for improving the biological efficacy of ATZ, a set of eight new ruthenium–ATZ complexes ($RuCl_2$ATZCOD, COD is 1,5-cyclooctadiene) were prepared, chemically and biologically characterized, including in vitro assays against epimastigotes and trypomastigote forms of the parasite and also assessment of cytotoxicity in mammals. Two of these complexes presented antitrypanosomal activity at non-cytotoxic concentrations on mammalian cells and of higher potency than its metal–free ligands, while the metallic precursor [$RuCl_2$COD$(MeCN)_2$] showed only moderate antitrypanosomal activity. Comparative analysis between the ruthenium complexes and metal–free ligands demonstrated the usefulness of this approach, with the establishment of new SAR data. Additional pharmacological tests, including a DNA bond assay, gave rise to the proposal of a single preliminary explanation for the molecular origin of the bioactivity.

1. Introduction

Trypanosoma cruzi, the parasitic protozoan agent of Chagas' disease or American trypanosomiasis, affects about 17 million people, and around 100 million people are at risk of infection across Latin America.[1] *T. cruzi* infection results in a generally mild acute phase, followed by a relatively long but asymptomatic 'indeterminate' phase, while it is estimated that around 30% of infected patients will develop the symptomatic chronic phase of Chagas' disease, which is characterized by the presence of myocarditis (often called chagasic cardiomyopathy) and in some cases, pathological disorders of the peripheral nervous and gastrointestinal systems.[2,3] Benznidazole (Rochagan®) is the only chemotherapeutic agent used for the treatment of Chagas patients, but it is highly toxic and of limited efficacy during the chronic phase of the disease.[4] There is thus great interest in developing novel approaches and targets for anti-*T. cruzi* drug design.

On the one hand, several biochemical pathways of fundamental importance (e.g., sterol biosynthesis[5] and pyrophosphate metabolism[6]) and validated targets (e.g., cysteine protease cruzain,[7] trypanothione reductase,[8] *trans*-sialidase[9]) of *T. cruzi* have proved useful for more advanced designs of new anti-*T. cruzi* agents. On the one other hand, an important way of discovering new antitrypanosomal agents is structural optimization of validated lead compounds and also increasing the 'drugability',[10] exploring useful medicinal chemistry concepts, such as bioisosterism,[11] molecular hybridization,[12] applying pharmacophore models,[13] in addition to the complexation of transition metals with bioactive ligands.[14]

A significant number of studies have provided evidence of the usefulness of applying the complexation of transition metals with antitrypanosomal ligands as a strategy for enhancing pharmacological properties (efficacy, bioavailability) or the desired chemical properties (such as the lipophilicity, reactivity).[15] The DNA structure was the first recognized target[14] for the antitrypanosomal metal complexes, although, more recently, other *T. cruzi* targets that interact with metal complexes have been discovered, such

* Corresponding authors. Tel.: +55 81 3341 8511; fax: +55 81 2126 8510 (A.C.L.L.).
E-mail addresses: cdonnici@terra.com.br (C.L. Donnici), ana.leite@pq.cnpq.br (A.C.L. Leite).

0968-0896/$ - see front matter Crown Copyright © 2009 Published by Elsevier Ltd. All rights reserved.
doi:10.1016/j.bmc.2009.05.071

as the cysteine protease cruzain,[16] trypanothione reductase,[17] NADH-fumarate reductase[18] and also affecting the nitric oxide level.[19]

Among the transition metals, ruthenium has proved to be an excellent choice for the development of anti-*T. cruzi* metal complexes, as illustrated briefly in Figure 1, because of their redox stability, excited state lifetime and rate of ligand exchange. For example, Ru(II) complexes of ketoconazole,[20] clotrimazole[20] or benznidazole[21] are more potent when compared with free bioactive ligands in inhibiting *T. cruzi* cell cultures.

In our previous studies, a congener series of aryl-4-oxothiazolylhydrazones (ATZ) was designed as antitrypanosomal agents. The in vitro pharmacological results indicated that, although effective in inhibiting epimastigotes (proliferative form) at micromolar range and of low cytotoxicity in mammals, the majority of ATZ derivatives displayed only moderate to poor activity against trypomastigotes (bloodstream form) of *T. cruzi*.[22] In fact, although of limited efficacy, this family of compounds is endowed with some of the desired biological and chemical features—low cytotoxicity, non-nitrated, non-peptide, and chemically tractable—and thus represent an attractive scaffold for the design of antitrypanosomal agents.

From the point of view of medicinal chemistry, the AZT are deemed to be non-classical bioisosters[11] of thiosemicarbazones, and much effort has been devoted to studying the structure–activity relationships (SAR) of metal–thiosemicarbazone complexes,[23] although, there is no report in the literature of complexation of AZT with ruthenium or with other transition metals, with the exception of a few examples involving organometallic compounds.[24] Furthermore, sulfur-based ligands have been shown to display the desired pharmacological features and have subsequently attracted special attention.[25]

Considering the bioinorganic approach to be one possible strategy for enhancing the pharmacological profile of ATZ ligands, in this study we describe the preparation and biological characterization of eight new ruthenium complexes with ATZ ligands [$RuCl_2$(ATZ)(COD)], where COD represents 1,5-cyclooctadiene. We chose COD as the second ligand, because this ligand possesses remarkable ability to interact with biological targets by way of hydrophobic interaction and also provides chemical stability throughout the Ru complexes.[26,27] Furthermore, to get an insight into the mechanism of action, studies of DNA interaction and more elaborate parasite inhibition tests were performed for selected Ru complexes.

2. Results

2.1. Chemistry

The ruthenium complexes were obtained by reaction of one equivalent of the metallic precursor $[RuCl_2(\eta^4\text{-}C_8H_{12})(MeCN)_2]$[28] with one equivalent of the respective **ATZ1–8** ligand in methanol under reflux. All these complexes were fully characterized using chemical analysis and spectroscopic data. The elemental analysis (C, H and N) data accorded well with the calculated values. The ^{1}H NMR spectra of the complexes were consistent with their corresponding protons both in terms of chemical shifts and the number of hydrogen atoms, in accordance with the proposed formula. More specifically, the CH=N protons of the complexes resonated at 10.9–11.9 ppm as a singlet, owing to a deshielding effect observed for those protons that are in close proximity to the coordinating atoms (azomethynic nitrogen), while, on free ligands, CH=N protons resonated at 6.9–7.8 ppm.

The ^{13}C NMR spectra revealed the presence of the expected number of signals corresponding to different types of carbon atoms present in the complexes. In this analysis, eight well-resolved resonance peaks were observed, which also showed that the carbons on the COD ligand coordinated with ruthenium were nonequivalent. The signals arising from azomethine carbon (CR=N) underwent an upward shift and occurred at δ 157–162 ppm, and also provide proof that nitrogen is involved in coordination. Assignment of each individual band to a specific vibration of IR spectra was attempted. The strong bands at (1635–1637 cm^{-1}) were observed in all the complexes, which are attributable to the chelation of (νCR=N) with metal. By contrast, the (νCR=N) bands for the free ligands are generally of higher frequency (1640–1645 cm^{-1}) and are of weaker intensity than those observed in the Ru complexes. In addition to this, bands in the low wavenumber region for the ruthenium complexes that may be tentatively attributed to (νRu–N, νRu–S) were observed. These are of importance in confirming that the sulfur atom is involved in the sphere of coordination. These spectra data allow it to be concluded that an N,S-bidentate coordination is involved in these complexes, as proposed in Scheme 1. All the complexes were soluble in methanol, DMSO, dichloromethane, chloroform and acetonitrile, producing intense yellow or brown solutions.

2.2. Pharmacology

All complexes were tested in vitro against the epimastigote (proliferative form) and trypomastigote (bloodstream form) of *T. cruzi* (Y strain) and also for cytotoxicity using BALB/c mouse splenocytes. Lymphocytes, which are the most abundant type of cells present in spleen cells, constitute a highly susceptible group of cells and this is, therefore, a suitable method for carrying out the cytotoxicity tests.[29] The anti-*T. cruzi* properties were expressed in terms of the IC_{50} (μM) values, the cytotoxicity being expressed as the highest concentration tested that was not cytotoxic for the splenocytes. Benznidazole (**Bdz**) and Nifurtimox (**Nfx**) were used as the reference antitrypanosomal drugs. All free ligands were previously subjected to a biological assay using the same technique for epimastigote and trypomastigote forms of *T. cruzi*,[22] and structure–

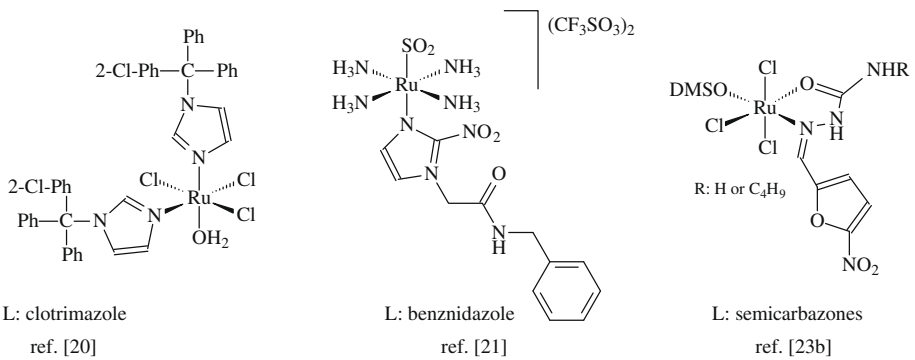

Figure 1. Selected ruthenium complexes endowed with antitrypanosomal activities. For these examples, bioactive ligands (L) were employed.

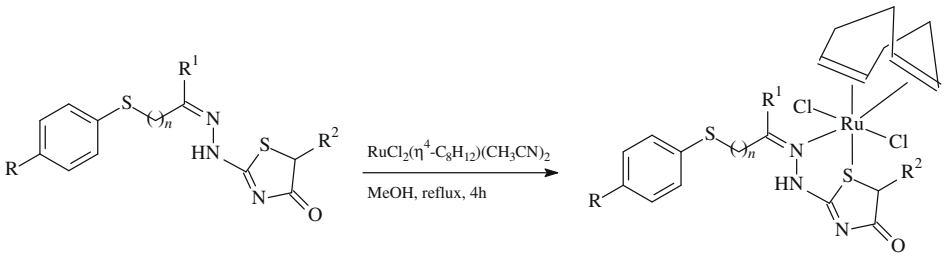

ATZ1: R=H, R_1=H, R_2=H, n=1
ATZ2: R=H, R_1=H, R_2=C_2H_5, n=1
ATZ3: R=H, R_1=H, R_2=H, n=2
ATZ4: R=H, R_1=CH_3, R_2=CH_3, n=1
ATZ5: R=CH_3, R_1=H, R_2=CH_3, n=1
ATZ6: R=CH_3, R_1=H, R_2=H, n=1
ATZ7: R=Cl, R_1=H, R_2=H, n=1
ATZ8: R=Br, R_1=H, R_2=H, n=1

R-ATZ1: R=H, R_1=H, R_2=H, n=1
R-ATZ2: R=H, R_1=H, R_2=C_2H_5, n=1
R-ATZ3: R=H, R_1=H, R_2=H, n=2
R-ATZ4: R=H, R_1=CH_3, R_2=CH_3, n=1
R-ATZ5: R=CH_3, R_1=H, R_2=CH_3, n=1
R-ATZ6: R=CH_3, R_1=H, R_2=H, n=1
R-ATZ7: R=Cl, R_1=H, R_2=H, n=1
R-ATZ8: R=Br, R_1=H, R_2=H, n=1

Scheme 1. Preparation of ruthenium complexes.

activity relationships (SARs) will be qualitatively discussed using the chemical group of ligands and comparison of Ru complexes with their corresponding free ligands. For the purposes of comparison, the antitrypanosomal properties of the metallic precursor [$RuCl_2(\eta^4\text{-}C_8H_{12})(MeCN)_2$] were tested, so as to establish a point of reference for the ruthenium entity (Table 1).

3. Discussion

First, the **R-ATZ1**, which possesses the non-substituted ligand **ATZ1**, showed IC_{50} values of 3.8 and 6.2 μM against epimastigote and trypomastigote forms of *T. cruzi*, respectively, whereas that **ATZ1** ligand displayed significant activity only against the trypomastigote form, with IC_{50} = 7.8 μM. By contrast, the metallic precursor was only able to inhibit the proliferation of epimastigotes, although with lower potency than the **R-ATZ1** complex and the reference drugs, **Nfx** and **Bdz**. As for the more liposoluble **ATZ2** and **ATZ3** ligands, their **R-ATZ2** and **R-ATZ3** complexes did not display enhanced potency against the epimastigote form. However, these two complexes showed activity against the trypomastigote form, as exemplified by the **R-ATZ2** complex, which was nine times more potent than free ligand **ATZ2**.

Table 1
In vitro biological characterization of ATZ ligands and their ruthenium complexes

Compd	IC_{50} (μM)[a] *Trypanosoma cruzi*, Y strain		Cytotoxicity (μg mL^{-1})[b]
	Trypomastigotes at 24 h	Epimastigotes at 11 days	
ATZ1	7.8	35.0	>100
R-ATZ1	6.2	3.8	1 (1.4)
ATZ2	48.2	0.3	>100
R-ATZ2	5.0	8.1	1.0
ATZ3	10	2.9	>100
R-ATZ3	6.4	10.9	1.0
ATZ4	Nd	83.3	>100
R-ATZ4	27.2	87.2	1.0
ATZ5	84.8	63.4	>100
R-ATZ5	7.0	11.4	1.0
ATZ6	20	92.3	>100
R-ATZ6	5.3	6.4	2 (4.5)
ATZ7	82.4	43.9	>100
R-ATZ7	3.3	2.4	1.0 (1.7)
ATZ8	Nd	42.9	>100
R-ATZ8	5.5	1.8	5.0 (8.0)
$RuCl_2(\eta^4\text{-}C_8H_{12})(MeCN)_2$	Nd	12.7	1.0 (1.4)
Bdz[c]	5.0	6.6	25
Nfx[c]	8.5	1.9	1.0 (3.4)

[a] Calculated at seven concentrations using data obtained from at least three independent experiments, with a SD less than 10% in all cases.
[b] Expressed as the highest concentration tested that was not cytotoxic for the BALB/c mice splenocytes. Values in μM are showed in parentheses.
[c] Bdz, Benznidazole and Nfx, Nifurtimox. Nd is not determined at tested concentrations.

The **R-ATZ6**, **R-ATZ7** and **R-ATZ8** complexes, designed using three congener ligands, were able to reduce the growth of the parasite at concentrations well below 10 μM, showing a potency similar to that of **Bdz** and **Nfx**. The efficacy of these complexes against the trypomastigote form was more remarkable when compared with their respective **ATZ6**, **ATZ7** and **ATZ8** ligands. Furthermore, an interesting trend was observed in these three complexes: the **R-ATZ8** and **R-ATZ7** (ligands with a *p*-bromo or *p*-chloro substituent, respectively) were three times more potent than the **R-ATZ6** complex (ligand with a *p*-methyl substituent). However, the majority of complexes showed an undesired range of cytotoxicity in mammals, and only the **R-ATZ8** complex displayed antitrypanosomal properties at concentrations that are not cytotoxic for mammalian cells. This represents the kind of profile that is generally required for antiparasitic agents acting against parasites over mammalian counterpart.

It is also worth commenting further on the role of substituents attached to ligands located near the coordination sphere. Varying the substituents produces the following order of potency: **R-ATZ6** > **R-ATZ5** ≫ **R-ATZ4**. Analysis of the ligand structures for these three complexes revealed that attaching a methyl at the R2 position (**R-ATZ5**) marginally decreases potency in comparison to **R-ATZ6**. In addition, the displacement of the methyl from the R (**R-ATZ5**) to R1 position (**R-ATZ4**) results in remarkable loss of potency. These results thus provide an insight regarding the impact of the presence of a substituent on a ligand located very near to atoms involved in the coordination sphere with ruthenium on antitrypanosomal activity (Scheme 2). In other words, this probably occurs as a result of some kind of steric changes that affect the geometry of complexes, resulting in the distinguishable process of recognition by or affinity with parasite targets.

With regard to the manner that the drugs act against the *T. cruzi* parasite, which may be trypanostatic (i.e., merely delaying parasite replication) or trypanocidal (effectively killing the parasite), analysis of the time–response curves during the antitrypanosomal assay revealed that two complexes (**R-ATZ7** and **R-ATZ8**) inhibited epimastigote replication at day 13 after completion of treatment, this being very similar to **Bdz**, which is described as a trypanocidal drug.[4a] This biological performance suggests that the Ru complexes are probably trypanocidal agents.

To ascertain whether complexation with a ligand is an essential factor for antitrypanosomal activity, the same culture of trypom-

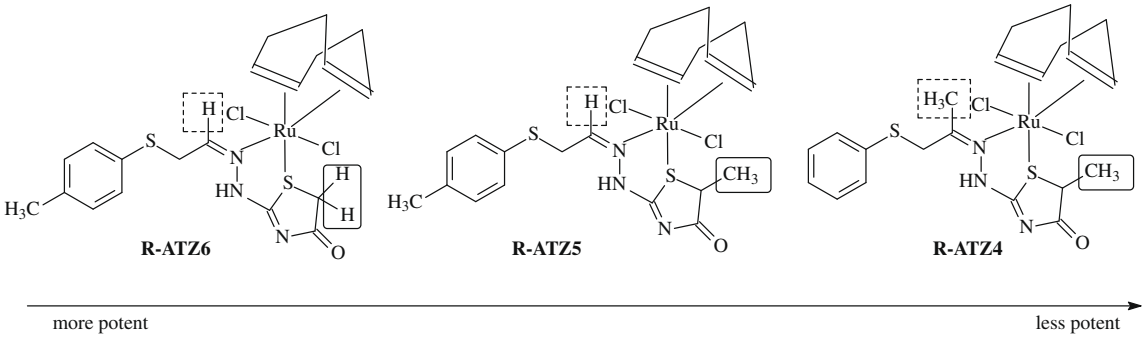

Scheme 2. The influence of substituents around the ligand structures on antitrypanosomal activity.

astigotes was simultaneously treated with stoichiometric quantities of metal–free ligand **ATZ8** and metallic precursor $[RuCl_2(\eta^4\text{-}C_8H_{12})(MeCN)_2]$, with IC_{50} being measured after 24 h of treatment. In this short test, the IC_{50} value was 15.4 μM, approximately three times higher than that of the corresponding **R-ATZ8** complex (IC_{50} = 5.5 μM). This key finding provides evidence that the formation of the metal complex plays a crucial role in determining the antitrypanosomal properties, rather than the simple presence of the ligand or ruthenium alone.

Research into kinetoplastid parasite targets have provided evidence that damage to DNA (affecting the topology and organization of intracellular DNA) or the inhibition of DNA topoisomerases (affecting the replication of DNA) provide a tool for preferentially killing the highly replicative parasite cells within the host.[30] To acquire greater understanding of the antiprotozoal activity, we performed one short assay of DNA interaction using plasmid DNA, which was carried out under agarose gel electrophoresis. For this assay, we chose the **R-ATZ8** complex**,** which is one of the most selective of such complexes, with a view to comparing it with the metallic precursor $[RuCl_2(\eta^4\text{-}C_8H_{12})(MeCN)_2]$. The ruthenium complex, **R-ATZ8**, shows a concentration-dependent ability to modify the migration and relative proportions of the plasmid DNA conformation (Fig. 2), while such effects are not observed in the case of free ligand **8** (data not shown). In the case of $[RuCl_2(\eta^4\text{-}C_8H_{12})(MeCN)_2]$, the strongest effect on conformation changes in plasmid DNA was observed as soon as a concentration of 10 μM was reached. The data therefore suggest that the DNA structure may constitutes one of targets used by ruthenium complexes to produce anti-*T. cruzi* effects.

A survey of the literature shows that the ligand exchanges in ruthenium-based drugs represent a crucial pathway in the biological activity.[31] In light of these studies, it seems appropriate to propose that a loss or exchange of chlorine ligands may occur in the complexes described here, providing a means for drug activation or formation of reactive species that can covalently interact with biomacromolecules.

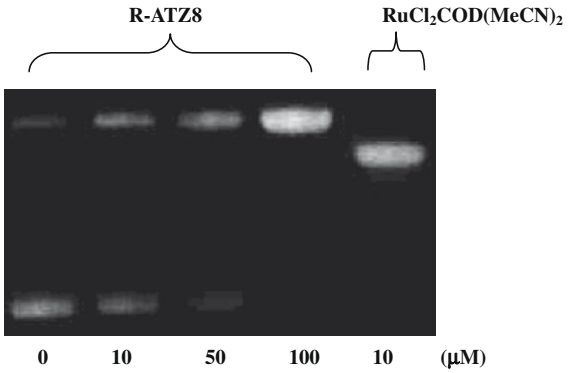

Figure 2. Effect of increasing concentrations of complex **R-ATZ8** on plasmid DNA. All reactions were incubated in 10 μM Tris–HCl (pH 7.4) to a final volume of 20 μL, and incubated for 24 h at 37 °C. The concentrations used (μM) are given at the bottom of gel section. The metallic precursor $[RuCl_2COD(MeCN)_2]$ was used as the point of reference.

4. Conclusions

We have demonstrated that the complexation of bioactive ligands with ruthenium leads to a new set of anti-*T. cruzi* agents with an attractive range of efficacy against the aforementioned parasite. Structure–activity relationships between the ligands and complexes were successfully determined by comparing IC_{50} values. The combined data from pharmacological tests are consistent with the conclusion that the **R-ATZ8** complex constitutes an example of a prototype of antitrypanosomal drug. The action mechanism must, in part, be related to action on the DNA structure. Obviously, is to be expected that other biological properties of the free ligands may have been modified subsequent to metal coordination and further investigations will describe this in due course.

5. Experimental

5.1. Chemistry

All common laboratory chemicals were purchased from commercial sources and used without further purification. Melting points were determined using a Thomas Hoover apparatus and are uncorrected. FTIR spectra were obtained using a Perkin Elmer 283B spectrometer in the range of 150–4000 cm^{-1} (KBr pellets) and at 150–700 cm^{-1} (as polyethylene pellets). ^1H NMR and ^{13}C NMR spectra were measured on a Bruker 200 MHz NMR spectrometer (at 200 MHz for ^1H and 60 MHz for ^{13}C) using $CDCl_3$ as solvent and TMS as an internal standard. Coupling constants (J) are given in hertz. Splitting patterns are designated as follows; s, singlet; d, doublet; t, triplet; m, multiplet. In the NMR data, COD represents 1,5-cyclooctadiene and Het thiazole heterocyclic. Elemental analyses were performed on a PE-2400 instrument for C, H, and N and the results lay within the acceptable range (±0.4%). The $[RuCl_2(\eta^4\text{-}C_8H_{12})(CH_3CN)_2]$ complex was prepared in accordance the procedure outlined in the literature,[28] using $RuCl_3$ as the initial metal source. All ATZ ligands were synthesized as previously reported[22] and obtained in the form of a racemic mixture for the chiral products.

5.1.1. General procedure for synthesis of ruthenium complexes[23a]

A solution of aryl-4-oxothiazolylhydrazone (0.001 mol) in dry methanol (10 mL) was added to a Schlenk flask containing a magnetically stirred solution of [Ru(η^4-C_8H_{12})($CH_3CN)_2Cl_2$)] (0.001 mol) in hot dry methanol (10 mL) in a water bath. After heating and magnetic stirring under reflux for 4 h, the obtained solution turns orange. The reaction flask was then agitated at room temperature for 2 h and a yellowish solid precipitate obtained. After filtration, washing with cold methanol and drying in a vacuum at room temperature, the pure complex was obtained in medium yields.

5.1.1.1. Dichloro [2-(phenylthio-(*Z*)-ethylidene)hydrazone-1,3-thiazol-4(5*H*)-one] cyclooctadiene ruthenium(II) (R-ATZ1). Greenish solid; yield: 49%; dec. temp. 215 °C (from methanol). Anal. Calcd for $C_{19}H_{23}N_3OS_2Cl_2Ru$: C, 41.83; H, 4.25; N, 7.70. Found: C, 41.87; H, 4.27; N, 7.73. UV–vis (cm^{-1}): ν 22,010, 36,736, 49,419. IR (ν_{max}, cm^{-1}): 3170 (NH), 1710 (C=O), 1635–1600 (C=N), 1000 (C–S), 539, 505, 489 (Ru–N, Ru–S). ^{1}H NMR ($CDCl_3$, δ, ppm): 10.9 (1H, s, –CH=N), 7.4–7.0 (5H, m, aryl), 7.38 (1H, s, NH), 4.6–4.5 (2H, m, =CHCOD), 4.1–3.9 (6H; 2H of CH=COD; 2H of CH_2Het, 2H, of CH_2–S), 2.6–2.5 (4H, m, *exo* CH_2), 2.2–2.1 (4H, m, *endo* CH_2). ^{13}C NMR ($CDCl_3$, ppm) δ 181.1 (C=O), 168.8 (C=N), 158.4 (CH=N), 130.6, 129.3, 129.1, 127.1, 98.9, 91.7, 89.3, 86.1, 83.09, 39.1 (Ar-S–CH_2), 32.1, 28.2, 28.1, 28.0.

5.1.1.2. Dichloro [2-(phenylthio-(*Z*)-ethylidene)hydrazone-5-ethyl-1,3-thiazol-4(5*H*)-one] cyclo octadiene ruthenium(II) (R-ATZ2). Green solid; yield: 41%; dec. temp. 185 °C (from methanol). Anal. Calcd for $C_{21}H_{27}N_3OS_2Cl_2Ru$: C, 43.98; H, 4.75; N, 7.33. Found: C, 44.07; H, 4.70, N, 7.40. UV–vis (cm^{-1}): ν 22,012, 36,740, 49,418. IR (ν_{max}, cm^{-1}): 3165 (NH), 1705 (C=O), 1635, 1600 (C=N), 1000 (C–S), 499, 484, 468 (Ru–N, Ru–S). ^{1}H NMR ($CDCl_3$, ppm) δ 11.9 (1H, s, CH= N), 7.56 (1H, s, NH), 7.2–7.1 (5H, m, aryl), 4.6–4.2 (4H, m, =CHCOD), 3.34 (1H, m, CH), 3.58 (2H, d, CH_2Het); 2.6–2.5 (4H, m, *exo* CH_2), 2.2–2.1 (4H, m, *endo* CH_2), 1.80 (2H, m, CH_2), 1.11 (3H, t, CH_3). ^{13}C NMR ($CDCl_3$, ppm) δ 183.54 (C=O), 175.2 (C=N), 162.0 (CH=N), 156.6, 131.8, 131.7, 131.3, 129.9, 98.6, 97.2, 91.2, 82.8, 51.2 (Ar-S–CH_2), 49.1, 39.3 (CH_2-Het), 33.9, 31.9, 27.9, 11.2 (CH_3).

5.1.1.3. Dichloro [2-(phenylthio-(*Z*)-propylide-ene)hydrazone-1,3-thiazol-4(5*H*)-one] cycloocta diene ruthenium(II) (R-ATZ3). Yellow solid; yield: 49%; dec. temp. 225 °C (from methanol). Anal. Calcd for $C_{20}H_{25}N_3OS_2Cl_2Ru$: C 42.93; H, 4.50; N, 7.51. Found: C, 42.97, H, 4.56, N, 7.50. UV–vis (cm^{-1}): ν 22,011, 36,739, 49,420. IR (ν_{max}, cm^{-1}): 3171 (NH), 1711 (C=O), 1636, 1600 (C=N), 1001 (C–S), 540, 506, 490 (Ru–N, Ru–S); ^{1}H NMR ($CDCl_3$, ppm) δ 10.8 (1H, s, –CH= N), 7.5–7.3 (6H; 5H, m, aryl; 1H, s, NH), 4.7–4.6 (4H, m, =CH COD), 3.94 (2H, CH_2Het), 3.1–3.0 (6H, 4H, *exo* CH_2COD and 2H, CH_2); 2.3–1.9 (6H; 4H, *endo* CH_2COD and 2H of CH_2–CH=N). ^{13}C NMR ($CDCl_3$, ppm) δ 180.4 (C=O), 177.7 (C=N), 159.8 (CH=N), 130.5, 129.8, 129.1, 129.1, 95.7, 91.3, 89.9, 85.4, 38.3 (CH_2–S-Ar), 34.0 (CH_2-Het), 32.2 (*C*H_2–CH=N), 29.6, 26.6, 28.5, 28.1.

5.1.1.4. Dichloro [2-(phenylthio-(*Z*)-propylide-2-ene)hydrazone-5-methyl-1,3-thiazol-4(5*H*)-one] cyclooctadiene ruthenium(II) (R-ATZ4). Light-yellow solid; yield: 48%; dec. temp. 287 °C (from methanol). Anal. Calcd for $C_{21}H_{27}N_3OS_2Cl_2Ru$: C, 43.98; H, 4.74; N, 7.33. Found: C, 44.07, H, 4.70, N, 7.40. UV–vis (cm^{-1}): ν 22012, 36738, 49420. IR (ν_{max}, cm^{-1}): 3165 (NH), 1707 (C=O), 1635–1600 (C=N), 1002 (C-S), 498, 485, 469 (Ru-N, Ru-S). ^{1}H NMR ($CDCl_3$, ppm): δ 10.9 (1H, t, =CHN), 7.5–7.2 (5H, m, aryl), 7.58 (1H, s, NH), 4.50 (1H, q, CH), 4.3–4.2 (4H, m, =CHCOD); 3.58 (2H, d, CH_2); 2.6-2.5 (4H, m, *exo* CH_2), 2.45 (3H, s, CH_3–C=N); 2.2–2.1 (4H, m, *endo* CH_2); 1.65 (d, 3H, CH_3). ^{13}C NMR ($CDCl_3$, ppm): δ 183.0 (C=O), 163.5 (CH_3C=N), 134.0, 132.5, 128.1, 88.7, 87.7, 85.1, 84.9, 49.3 (*C*H_2–S-Ar), 47.8 (*C*H_2–CH=N), 47.5 (CH_2-Het), 33.2, 32.8, 31.6, 27.4, 20.9, 19.9, 16.9 (CH_3).

5.1.1.5. Dichloro [2-(*para*-methylphenylthio-(*Z*)-ethylidene)hydrazone-5-methyl-1,3-thiazol-4(5*H*)-one] cyclooctadiene ruthenium(II) (R-ATZ5). Greenish solid; yield: 45%; dec. temp. 217 °C (from methanol). Anal. Calcd for $C_{21}H_{27}N_3OS_2Cl_2Ru$: C, 43.98; H, 4.74; N, 7.33. Found: C, 44.07, H, 4.70, N, 7.40. Found: C, 44.10; H, 4.66; N, 7.44. UV–vis (cm^{-1}): ν 22,009, 36,738, 49,421. IR (ν_{max}, cm^{-1}): 3166 (NH), 1707 (C=O), 1635, 1601 (C=N), 1000 (C–S), 498, 483, 469 (Ru–N, Ru–S). ^{1}H NMR ($CDCl_3$, ppm) δ 11.0 (1H, =CHN), 7.2–7.1 (4H, m, aryl), 7.56 (1H, s, NH), 4.6–4.5 (4H, m, =CHCOD), 4.48 (1H, q, CH), 3.68 (2H, s, CH_2), 2.6–2.5 (4H, m, *exo* CH_2), 2.2–2.1 (4H, m, *endo* CH_2), 2.09 (3H, s, CH_3), 1.26 (3H, d, CH_3Het). ^{13}C NMR ($CDCl_3$, ppm) δ 184.3 (C=O), 161.9 (C=N), 159.3 (CH=N), 156.6, 146.3, 137.3, 131.7, 131.9, 130.1, 110.0, 96.1, 91.0, 90.9, 68.7, 51.2 (CH_2–S-Ar), 49.1 (CH_2-Het), 27.9, 21.4 (CH_3), 16.9 (CH_3).

5.1.1.6. Dichloro [2-(*para*-methylphenylthio-(*Z*)-ethylidene)hydrazone-1,3-thiazol-4(5*H*)-one] cyclooctadiene ruthenium(II) (R-ATZ6). Greenish solid; yield: 51%; dec. temp. 205 °C (from methanol). Anal. Calcd for $C_{20}H_{25}N_3OS_2Cl_2Ru$: C, 42.93; H, 4.50; N, 7.51. Found: C, 42.98; H, 4.55; N, 7.48. UV–vis (cm^{-1}): ν 22,009, 36,735, 49,418. IR (ν_{max}, cm^{-1}): 3169 (NH), 1708 (C=O), 1635, 1604 (C=N), 1001 (C–S), 535, 498, 483 (Ru–N, Ru–S). ^{1}H NMR ($CDCl_3$, ppm) δ 11.9 (1H, s, CH=N), 7.2–7.1 (4H, m, aryl), 7.58 (1H, s, NH), 4.31 (4H, d, CH_2), 4.6–4.5 (4H, m, =CHCOD), 2.6–2.5 (4H, m, *exo* CH_2), 2.1–2.2 (4H, m, *endo* CH_2); 2.18 (3H, s, CH_3). ^{13}C NMR ($CDCl_3$, ppm) δ 178.9 (C=O), 168.3 (C=N), 157.7 (CH=N), 131.5, 131.1, 130.1, 129.5, 98.7, 89.9, 86.1, 83.1, 39.4 (CH_2–S-Ar), 36.4 (CH_2-Het), 34.3, 33.8, 28.9, 24.5, 21.4 (CH_3).

5.1.1.7. Dichloro [2-(*para*-chlorophenylthio-(Z)-ethylidene)hydrazone-1,3-thiazol-4(5*H*)-one] cyclooctadiene ruthenium(II) (R-ATZ7). Light-green solid; yield: 65%; dec. temp. 204 °C (from methanol). Anal. Calcd for $C_{19}H_{22}N_3OS_2Cl_3Ru$: C, 39.35; H, 3.82; N, 7.25. Found: C, 39.41, H, 3.86, N, 7.31. UV–vis (cm^{-1}): ν22,011, 36,737, 49,418. IR (ν_{max}, cm^{-1}): 3165 (NH), 1705 (C=O), 1635, 1600 (C=N), 1000 (C–S), 499, 484, 468 (Ru–N, Ru–S). ^{1}H NMR ($CDCl_3$, ppm) δ 11.8 (1H, s, CH=N), 7.3–7.2 (4H, m, aryl), 7.56 (1H, s, NH), 4.6–4.5 (4H, m, =CHCOD); 4.0–3.8 (2H, CH_2), 3.58 (2H, d, CH_2Het); 2.6–2.5 (4H, m, *exo* CH_2), 2.2-2.1 (4H, m, *endo* CH_2). ^{13}C NMR ($CDCl_3$, ppm) δ 180.9 (C=O), 168.9 (C=N), 158.5 (CH=N), 157.7, 133.3, 132.1, 129.6, 110.0, 98.9, 89.5, 83.1, 39.0 (CH_2-S-Ar), 34.0 (CH_2-Het), 33.1, 32.0, 30.7, 28.9.

5.1.1.8. Dichloro[2-(*para*-bromophenylthio-(*Z*)-ethylidene)hydrazone-1,3-thiazol-4(5*H*)-one] cyclooctadiene ruthenium(II) (R-ATZ8). Yellowish solid; yield: 58%; dec. temp. 204 °C (from methanol). Anal. Calcd for $C_{19}H_{22}N_3OS_2BrCl_2Ru$: C, 36.55; H, 3.55; N, 6.73. Found: C, 36.59; H, 3.60; N, 6.70. UV–vis (cm^{-1}): ν 22,011, 36,740, 49,420. IR (ν_{max}, cm^{-1}): 3167 (NH), 1705 (C=O), 1637, 1602 (C=N), 1703 (C=O), 1002 (C–S), 499, 484, 468 (Ru–N, Ru–S). ^{1}H NMR ($CDCl_3$, ppm): δ 11.7 (1H, s, CH=N), 7.2–7.1 (4H, m, aryl), 7.51 (1H, s, NH), 4.6–4.5 (4H, m, =CH COD); 4.0–3.8 (2H, s, CH_2), 3.58 (2H, d, CH_2Het); 2.6–2.5 (4H, m, *exo* CH_2), 2.2–2.1 (4H, m, *endo* CH_2). ^{13}C NMR ($CDCl_3$, ppm): δ 181.4 (C=O), 177.1, 176.0, 158.1 (CH=N), 133.9, 131.7, 130.8, 119.4, 101.1, 98.9, 94.2, 82.6, 39.7(CH_2–S-Ar), 38.2 (CH_2-Het), 31.2, 30.4, 28.0.

5.2. Pharmacological tests

5.2.1. In vitro cytotoxicity

The cytotoxicity of the complexes was determined using BALB/c mice splenocytes (5×10^6 cells·well^{-1}) cultured in 96-well plates in Dulbecco's Modified Eagle's Medium (DMEM, Sigma Chemical

Co., St. Louis, MO) supplemented with 10% of fetal calf serum (FCS; Cultilab, Campinas, SP, Brazil) and 50 μg mL^{-1} of gentamycin (Novafarma, Anápolis, GO, Brazil). Each compound was evaluated at five concentrations (1, 2, 5, 10, 25, 50, 100 μg mL^{-1}), in triplicate. Cultures were incubated in the presence of ^{3}H-thymidine (1 μCi $well^{-1}$) for 24 h at 37 °C and 5% CO_2. After this period, the content of the plate was harvested to determine ^{3}H-thymidine incorporation using a beta-radiation counter (LKB Wallac Rack Beta, Pharmacia Biotech). The cytotoxicity of the compounds was determined by comparing the percentage of ^{3}H-thymidine incorporation (as an indicator of cell viability) in drug-treated wells in comparison to untreated wells. Non-cytotoxic concentrations were defined as those causing a reduction of ^{3}H-thymidine incorporation below 10% in relation to untreated controls.

5.2.2. In vitro antiproliferative activity

Epimastigotes of *T. cruzi* (Y strain) were cultivated at 26 °C in Liver Infusion Tryptose medium (LIT) supplemented with 10% fetal calf serum, 1% hemin, 1% R9 medium and 50 μg mL^{-1} gentamycin. Parasites (10^6/cells/mL) were cultured in a fresh medium in the absence or in the presence of the compounds being tested (from stock solution in DMSO). Cell growth was determined after 11 days of culture by counting viable forms in a hemacytometer, in triplicate. The complexes used were from a stock solution in DMSO. To determine the IC_{50}, cultures of Y strain epimastigotes in the presence of different concentrations of the compounds were evaluated after 11 days as described above. IC_{50} calculation was carried out using non-linear regression on PRISM 4.0 GRAPHPAD software. Y strain *T. cruzi* trypomastigotes were obtained from culture supernatants of Vero cell line at 37 °C and placed in 96-well plates (4×10^5 $well^{-1}$) in a DMEM medium supplemented with 10% FCS and 50 μg mL^{-1} gentamycin. Viable parasites were counted in a hemacytometer 24 h after addition of complexes by way of trypan blue exclusion. The percentage of inhibition was calculated in relation to untreated cultures. The same procedure was performed for **Bdz** and **Nfx** (reference drugs) and vehicle alone, DMSO as blank.

5.2.3. DNA studies

The pUC119 plasmid DNA (300 μM) was combined with different concentrations (0–100 μM) of the ruthenium complex **R-8** previously dissolved in DMSO and diluted to the proper concentration using the Tris–HCl buffer. The samples were then incubated for 24 h (overnight) at 37 °C. During this time, appreciable hydrolysis or decomposition of the ruthenium complex was not detected by TLC. The reaction was then stopped by the addition of NaCl (1 M) to achieve a final chloride concentration of 0.2 M. 20 μL of each sample were run (100 V for 30 min.) in 1% agarose gel with 1 × TBE (containing 0.45 M Tris-HCl, 0.45 M boric acid, 20 μM EDTA, pH 8.0) and the reaction was stained with ethidium bromide. The bands were then viewed using a transluminator under UV light.

Acknowledgements

This study was supported by the Brazilian National Research Council (CNPq, Grants #DECIT-410401/2006-4 and #471834/2006-8), the State of Pernambuco Research Foundation (FACEPE, Grant #APQ-0123-4.03/08) and the State of Minas Gerais Research Foundation (FAPEMIG, Grants #EDT 479/07, #APQ-4911-5.02/07, #CEX 817/06). C. L. Donnici and M. H. Araújo are senior CNPq researchers and D. R. M. Moreira is PhD CNPq fellow. We gratefully acknowledge L. F. da Rocha and M. Nakazawa (CPqAM, FIOCRUZ) for technical assistance and A. Mattoy for her help in performing the DNA studies. V. R. A. Pereira would like to thanks Dr. Yara Gomes (CPqAM, FIOCRUZ) for kindly providing the Y strain of *Trypanosoma cruzi*.

References and notes

1. Coura, J. R. *Mem. Inst. Oswaldo Cruz* **2007**, *102*, 113.
2. Soares, M. B. P.; Pontes-De-Carvalho, L.; Ribeiro-dos-Santos, R. *An. Acad. Bras. Cienc.* **2001**, *73*, 547.
3. Antonio Marin-Neto, S. J.; Cunha-Neto, E.; Maciel, B. C.; Simões, M. V. *Circulation* **2007**, *115*, 1109.
4. (a) Coura, J. R.; Castro, S. L. *Mem. Inst. Oswaldo Cruz* **2000**, *97*, 3; (b) Urbina, J. A.; Docampo, R. *Trends Parasitol.* **2003**, *19*, 495.
5. Docampo, R.; Moreno, S. J. N. *Curr. Pharm. Des.* **2008**, *14*, 882.
6. Docampo, R.; Moreno, S. J. N. *Mol. Biochem. Parasitol.* **2001**, *33*, 151.
7. (a) Caffrey, C. R.; Scory, S.; Steverding, D. *Curr. Drug Targets* **2000**, *1*, 155; (b) Steverding, D.; Caffrey, C. R.; Sajid, M. *Mini-Rev. Med. Chem.* **2006**, *6*, 1025.
8. Krauth-Siegel, R. L.; Coombs, G. H. *Parasitol. Today* **1999**, *15*, 404.
9. Buschiazzo, A.; Tavares, G. A.; Campetella, O.; Spinelli, S.; Cremona, M. L.; Paris, G.; Amaya, M. F.; Frasch, A. C. C.; Alzari, P. M. *EMBO J.* **2000**, *19*, 16.
10. Congreve, M.; Carr, R.; Murray, C.; Jhoti, H. *Drug Discovery Today* **2003**, *8*, 876.
11. Lima, L. M.; Barreiro, E. J. *Curr. Med. Chem.* **2005**, *12*, 23.
12. (a) Viega-Junior, C.; Danuello, A.; Bolzani, V. S.; Barreiro, E. J.; Fraga, C. M. A. *Curr. Med. Chem.* **2007**, *14*, 1829; (b) Meunier, B. *Acc. Chem. Res.* **2008**, *41*, 69.
13. (a) Renner, S.; Schneider, G. *ChemMedChem* **2006**, *1*, 181; (b) Esch, I. J. P. D.; Mills, J. E.; Perkins, T. D.; Romeo, G.; Hoffmann, M.; Wieland, K.; Leurs, R.; Menge, W. M.; Nederkoorn, P. H.; Dean, P. M.; Timmermann, H. *J. Med. Chem.* **2001**, *44*, 1666.
14. Fricker, S. P. *Dalton Trans.* **2007**, 4903. and references cited therein.
15. For review of metal complexes as antiparasitic drugs see: Sanchez-Delgado, R. A.; Anzellotti, A. *Mini-Rev. Med. Chem.* **2004**, *4*, 23.
16. Fricker, S. P.; Mosi, R. M.; Cameron, B.; Baird, I.; Zhu, Y.; Anastassov, V.; Cox, J.; Doyle, P. S.; Hansell, E.; Lau, G.; Langille, J.; Olsen, M.; Qin, L.; Sherji, R.; Wong, R. S. Y.; Santucci, Z.; Mckerrow, J. H. *J. Inorg. Biochem.* **2008**, *102*, 1839.
17. Otero, L.; Vieites, M.; Boiani, L.; Denicola, A.; Rigol, C.; Opazo, L.; Olea-Azar, C.; Maya, J. D.; Morello, A.; Krauth-Siegel, R. L.; Piro, O. E.; Castelano, E.; Cerecetto, H.; Gambino, D.; Gonzalez, M.; Gambino, D. *J. Med. Chem.* **2006**, *49*, 3322.
18. Vieites, M.; Smircich, P.; Parajo-Costa, B.; Rodrıguez, J.; Galaz, V.; Olea-Azar, C.; Otero, L.; Aguirre, G.; Cerecetto, H.; Gonzalez, M.; Barrio, A. G.; Garat, B.; Gambino, D. *J. Biol. Inorg. Chem.* **2008**, *13*, 733.
19. Silva, J. J. N.; Osakabe, A. L.; Pavanelli, W. R.; Silva, J. S.; Franco, D. W. *Brit. J. Pharmacol.* **2007**, *152*, 112.
20. Navarro, M.; Lehmann, T.; Cisneros-Fajardo, E. J.; Fuentes, A.; Sanchez-Delgado, R. A.; Silva, P.; Urbina, J. A. *Polyhedron* **2000**, *19*, 2319.
21. Silva, J. J. N.; Pavanelli, W. R.; da Silva, A. B. F.; Silva, J. S.; Gutierrez, F. R. S.; Lima, F. C. A.; Franco, D. W. *J. Med. Chem.* **2008**, *51*, 4104.
22. Leite, A. C. L.; Moreira, D. R. M.; Cardoso, M. V. O.; Hernandes, M. Z.; Pereira, V. R. A.; Silva, R. O.; Kiperstok, A. C.; Lima, M. L.; Soares, M. B. P. *ChemMedChem* **2007**, *2*, 1339.
23. (a) Singh, S.; Athar, F.; Maurya, M. R.; Azam, A. *Eur. J. Med. Chem.* **2006**, *41*, 592; (b) Lucía Otero, L.; Aguirre, G.; Boiani, L.; Denicola, A.; Rigol, C.; Olea-Azar, C.; Maya, J. D.; Morello, A.; González, M.; Gambino, D.; Cerecetto, H. *Eur. J. Med. Chem.* **2006**, *41*, 1231; (c) Peres-Bebolledo, A.; Teixeira, L. R.; Batista, A. A.; Mangrich, A. S.; Aguirre, G.; Cerecetto, H.; Gonzalez, M.; Hernandez, P.; Ferreira, A. M.; Speziali, N. L.; Beraldo, H. *Eur. J. Med. Chem.* **2008**, *43*, 939; (d) Bernhardt, P. V.; Sharpe, P. C.; Islam, M.; Lovejoy, D. B.; Kalinowski, D. S.; Richardson, D. R. *J. Med. Chem.* **2009**, *52*, 407.
24. (a) Zhang, Z. *Appl. Organomet. Chem.* **2008**, *22*, 6; (b) Yu, H. B.; Shao, L.; Fang, J. X. *J. Organomet. Chem.* **2007**, *692*, 991.
25. (a) Sorasaenee, K.; Galán-Mascarós, J. R.; Dunbar, K. R. *Inorg. Chem.* **2002**, *41*, 433; (b) Huxham, L. A.; Cheu, E. L. S.; Patrick, B. O.; James, B. R. *Inorg. Chim. Acta* **2003**, *352*, 238; (c) Mosi, R.; Baird, I. R.; Cox, R.; Anastassov, V.; Cameron, B.; Skerji, R. T.; Fricker, S. P. *J. Med. Chem.* **2006**, *49*, 5262; (d) Bergamo, A.; Sava, G. *Dalton Trans.* **2007**, 1267.
26. Schmidt, K.; Jung, M.; Keilitz, R.; Schnurr, B.; Gust, R. *Inorg. Chim. Acta* **2000**, *306*, 6.
27. Sánchez-Delgado, R.; Navarro, M.; Perez, H.; Urbina, J. A. *J. Med. Chem.* **1996**, *39*, 1095.
28. Albers, M. O.; Ashworth, T. V.; Oosthuizen, H. E.; Singleton, E. *Inorg. Synth.* **1989**, *26*, 68.
29. Nogueira, R. C. N.; Oliveira-Costa, J. F.; de Sá, M. S.; dos Santos, R. R.; Soares, M. B. P. *Curr. Drug Targets* **2009**, *10*, 291.
30. (a) Das, A.; Dasgupta, A.; Sengupta, T.; Majumder, H. K. *Trends Parasitol.* **2004**, *20*, 381; (b) Fouce, R. B.; Redondo, C. M.; Pertejo, Y. P.; Gonzalez, R. D.; Reguera, R. M. *Drug Discovery Today* **2006**, *11*, 733; (c) Tse-Dinh, Y. C. *Infect. Disord: Drug Targets* **2007**, *7*, 3.
31. (a) Allardyce, C. S.; Dorcier, A.; Scolaro, C.; Dyson, P. J. *Appl. Organometal. Chem.* **2005**, *19*, 1; (b) Yan, Y. K.; Melchart, M.; Habtemariam, A.; Sadler, P. J. *Chem. Commun.* **2005**, 4764.